HUMAN GENE THERAPY 18:515–524 (June 2007)

DOI: 10.1089/hum.2006.162

In Vivo Imaging Shows Abnormal Function of Vascular Endothelial Growth Factor-Induced Vasculature

SERENA ZACCHIGNA,[1,2,*] ENNIO TASCIOTTI,[1,*] CLAUDIA KUSMIC,[3,*] NIKOLA ARSIC,[1] ORESTE SORACE,[3] CECILIA MARINI,[3] PAOLO MARZULLO,[3] SILVIA PARDINI,[3] DEBORA PETRONI,[3] LUCIA PATTARINI,[1] SILVIA MOIMAS,[1] MAURO GIACCA,[1] and GIANMARIO SAMBUCETI[3,4]

ABSTRACT

Although the angiogenic effect of vascular endothelial growth factor (VEGF) is widely recognized, a central question concerns whether the vessels formed on its overexpression effectively increase tissue perfusion *in vivo*. To explore this issue, here we exploit AAV vectors to obtain the prolonged expression of VEGF and angiopoietin-1 (Ang1) in rat skeletal muscle. Over a period of 6 months, muscle blood flow (MBF) and vascular permeability were measured by positron emission tomography and single-photon emission computed tomography, respectively. All measurements were performed under resting conditions and after electrically induced muscle exercise. Despite the potent angiogenic effect of VEGF, documented by vessel counting and intravascular volume assessment, the expression of this factor did not improve resting MBF, and it even decreased perfusion after exercise. This deleterious effect was related to the formation of leaky vascular lacunae, which accounted for the occurrence of arteriovenous shunts that excluded the downstream microcirculation. These effects were significantly counteracted by the coinjection of VEGF and Ang1, which determined a marked increase in resting MBF and, most notably, a significant improvement after exercise that persisted over time. Taken together, these results challenge the effectiveness of VEGF as a sole factor to induce angiogenesis and suggest the use of factor combinations to achieve competent vessel formation.

OVERVIEW SUMMARY

This paper exploits state-of-the-art positron emission tomography and single-photon emission computed tomography imaging techniques to visualize and measure tissue perfusion and vessel permeability in animals injected with adeno-associated viral vectors expressing VEGF or VEGF plus Ang1 over a period of 6 months. The results obtained indicated that VEGF expression, despite the histological evidence of neoangiogenesis, did not increase tissue perfusion and, in addition, it dramatically worsened perfusion after muscle exercise. This was due primarily to the increased permeability of the VEGF-induced vasculature and to the presence of arteriovenous shunts that excluded the microcirculation. Both deleterious effects were significantly counteracted by the simultaneous expression of Ang1. These results prompt caution in the use of VEGF as a sole factor to promote therapeutic neoangiogenesis.

INTRODUCTION

THE INDUCTION OF new blood vessel formation through the administration of growth factors remains a highly attractive option to promote the revascularization of otherwise untreatable ischemic tissues. Indeed, preclinical proof of concept of therapeutic angiogenesis has been extensively provided in several animal models and with the use of various therapeutic

[1]Molecular Medicine Laboratory, International Center for Genetic Engineering and Biotechnology, 34012 Trieste, Italy.
[2]Department of Biomedicine, University of Trieste, 34100 Trieste, Italy.
[3]Istituto di Fisiologia Clinica, Area della Ricerca del Consiglio Nazionale delle Ricerche, Pisa, Italy.
[4]Department of Internal Medicine, Institute of Nuclear Medicine, University of Genoa, 16132 Genoa, Italy.
*S.Z., E.T., and C.K. contributed equally to this work.

molecules (reviewed in Ferrara and Alitalo, 1999; Post and Waltenberger, 2005). However, in most instances the results obtained in clinical trials have been so far largely disappointing (Yla-Herttuala *et al*., 2004; Cao *et al*., 2005). It thus appears that the achievement of a meaningful therapeutic benefit for patients still requires the correct identification of the relevant factor or factor combinations able to trigger an effective angiogenic response, as well as the development of more efficient delivery vectors.

Early studies performed in various animal models have indicated that vascular endothelial growth factor (VEGF), by directly stimulating endothelial cell migration and proliferation, is able to trigger significant angiogenic capillary sprouting and neovascularization *in vivo* (Ferrara *et al*., 2003). In addition, prolonged expression of this factor also determines the massive formation of new arterioles, which have a diameter range from 20 to 120 μm and are connected to the systemic circulation (Arsic *et al*., 2003; Zentilin *et al*., 2006). We and others have observed that this powerful angiogenic and arteriogenic activity of VEGF provides clear benefit in improving vascularization in various experimental settings (Losordo *et al*., 1998; Schwarz *et al*., 2000; Deodato *et al*., 2002; Galeano *et al*., 2003; Zacchigna *et al*., 2005).

Despite the extensive evidence of new blood vessel formation in response to VEGF overexpression, available knowledge about the functionality of this newly formed vasculature is scanty. Indeed, this information is of particular relevance, because VEGF is also known to exert a powerful permeabilizing effect both *in vitro* and *in vivo* (Weis and Cheresh, 2005). In addition, a large body of evidence indicates that tumor-associated angiogenesis (which relies mainly on excessive VEGF production) generates poorly functional vessels (Ferrara, 2005). Altogether, these observations suggest that VEGF overexpression alone may not be sufficient to recapitulate the complexity of the events required for the whole angiogenic process, thus resulting in the formation of vessels of abnormal shape and leakiness.

Besides endothelial cell sprouting, the formation of a full-blown and functional vasculature requires the outward remodeling of the newly formed vessels, with the acquisition of a smooth muscle cell coat and the deposition of extracellular matrix. Angiopoietin-1 (Ang1) has been proven to be essential for proper vessel maturation and stabilization, by reinforcing endothelial cell connections, as well as by recruiting periendothelial cells (Thurston *et al*., 1999; Arsic *et al*., 2003). Therefore, the combination of VEGF and Ang1 has been proposed as a rational approach to induce the formation of a mature vasculature (Arsic *et al*., 2003; Siddiqui *et al*., 2003). Nevertheless, the functional outcome of such a combinatorial approach still remains unexplored.

Only a few gene therapy techniques are suitable for the delivery of cocktails of growth factors. Among these, viral vectors based on the adeno-associated virus (AAV) appear especially promising. In fact, these vectors transduce target cells at a high multiplicity of infection and are therefore suitable for the simultaneous administration of various gene combinations to the same cell. Moreover, two further features render these vectors particularly suitable for cardiovascular gene therapy. First, they show a specific tropism for quiescent cells, including skeletal muscle cells and cardiomyocytes; second, they ensure sustained and prolonged expression of transgenes *in vivo*, a desirable property to drive complex biological responses, including new blood vessel formation.

Here we exploit two AAV vectors to evaluate the functional competence of the vessels formed in response to the 165-amino acid isoform of VEGF ($VEGF_{165}$), administered either as a single factor or in combination with Ang1. Given that the aim of therapeutic neovascularization is to enhance perfusion and function of tissues, we assess muscle perfusion by positron emission tomography (PET) both under resting conditions and during a short period of pacing-induced intense muscle activity. We show that overexpression of VEGF alone not only is unable to enhance resting blood flow, but dramatically worsens muscle perfusion after exercise. We also provide two mechanisms that explain this negative effect, namely the increased permeability of the newly formed vasculature and the existence of arteriovenous shunts in the VEGF-treated muscles. Finally, we demonstrate that the simultaneous delivery of AAV-Ang1 is of significant therapeutic value, accounting for a marked improvement in muscle perfusion under resting conditions as well as after muscle activity.

MATERIALS AND METHODS

Production, purification, and characterization of recombinant AAV vectors

Three recombinant AAV (rAAV) vectors were used in this study, expressing the *lacZ* reporter gene and the cDNA for either the 165-amino acid isoform of VEGF (VEGF) or angiopoietin-1 (Ang1), under the control of the constitutive cytomegalovirus (CMV) immediate-early promoter. Vector stocks were prepared and titered as already described (Arsic *et al*., 2003, 2004). rAAV titers ranged from $\sim 1 \times 10^{12}$ to $\sim 1 \times 10^{13}$ viral genome units (VGU)/ml.

Animal and experimental procedures

Animal care and treatment were conducted in conformity with institutional guidelines, in compliance with national and international laws and policies (EEC Council Directive 86/609, OJ L 358, December 12, 1987). Eighty-four adult male Wistar rats weighing ~250 g were included in this study and housed under controlled environmental conditions. After mild general anesthesia, the right leg of each animal was injected with 400 μl of AAV vector (containing 4×10^{11} VGU); the left leg was injected with a similar volume of phosphate-buffered saline (PBS). Eight injections were performed in each leg: 2×50 μl into the tibialis anterior, 3×50 μl into the gastrocnemius, and 3×50 μl into the rectus femoris.

Measurement of flow response to muscular activity

Transmission maps were acquired in two-dimensional (2D) modality in anesthetized animals placed in the ring of a PET scanner (EXACT HR+; CTI Molecular Imaging/Siemens Medical Solutions, Malvern, PA), using an external source of ^{68}Ge before injection of 1–3 mCi of $^{13}NH_3$ in surgically exposed jugular vein. The tracer, diluted in 100 μl, was administered as a

bolus soon after the start of a dynamic acquisition (90 frames × 2 sec, 1 frame × 300 sec). One hour after the baseline studies, muscle contraction was induced by inserting two fine electrodes bilaterally into the tibialis anterior muscles followed by stimulation with an external pacemaker set to discharge square wave stimuli of 40 mA at a frequency of 120/min, for 15 min. After 12 min of exercise, a new dose of ammonia was injected and images were acquired.

Muscle blood flow through both hindlimbs was estimated by normalizing muscular uptake of ammonia for an index of tracer input function, according to the method described by Bellina and coworkers (1990). Briefly, a region of interest (ROI) was drawn on the cardiac area on the coronal plane and a time–concentration curve was obtained (see Fig. 2); this curve was fitted by a γ-variate function for integration. On the last equilibrium image, four ROIs were then drawn on each rat hindlimb, using a computer-based algorithm able to identify the somatic borders, to measure average muscle uptake of ammonia. The blood flow index for each limb was then obtained by the following equation:

$$\text{Muscular flow index} = \frac{\text{muscle ammonia uptake}}{\int_0^{\infty} \text{cardiac ammonia concentration}}$$

Measurement of vascular permeability and volume

Rats were positioned on the collimator of a γ-camera (GE Healthcare Technologies, Milwaukee, WI) equipped with a parallel hole, low energy–high resolution collimator. A bolus of diethylenetriaminepentaacetic acid (DTPA) labeled with 1 mCi of ^{99m}Tc was then injected into the jugular vein, simultaneously with the start of a dynamic acquisition of 300 one-second frames.

To calculate microvascular permeability, the method described by Peters and colleagues (1987) was used. In brief, the capillary permeability (x) surface product was estimated by the net early accumulation of ^{99m}Tc-DTPA, a tracer commonly used for renal scintigraphy and characterized by a molecular weight close to that of sucrose and by a low binding affinity for plasma proteins. According to this method, we identified the blood and tissue time–activity curve by positioning identical ROIs on the heart and on each hindlimb. Data collected during the first 50 sec after injection were then plotted, by placing the ratio M_a/H_a on the y axis and the function $\left[\int_0^t H_a(t) \times dt\right]/H_a(t)$ on the x axis, where H_a indicates the cardiac activity and M_a the activity in each hindlimb ROI, respectively.

The points of this relationship typically display a linear increase and can thus be fitted by linear regression analysis, identifying a regression line that can be described as follows:

$$\frac{M_a}{H_a} = \alpha \int_0^t H_a(t) \times dt + \beta$$

The slope a of this line represents the rate of DTPA clearance from the intravascular space into the extravascular compartment within the region of interest (see Fig. 4A). On the other hand, the intercept b represents an index of plasma volume (arterial, capillary, and venous combined) within this intravascular space. For each measurement, the ratio between control and treated hindlimb was considered.

Assessment of arteriovenous shunts

After completion of the follow-up, rats underwent surgical exposure of the abdominal aorta, under anesthesia and after heparinization (500 U administered intramuscularly). After identification of the renal arteries a minimum of 1×10^6 human albumin macroaggregates (GE Healthcare Technologies), ranging in diameter from 25 to 200 μm and labeled with a minimum of 3 mCi of ^{99m}Tc, was injected into the distal aorta.

Two minutes after injection, the animals were killed by anesthetic overdose, before the removal of the aortic needle, and placed on the head of a γ-camera (Millennium; GE Healthcare Technologies). The distribution of radioactivity was imaged in preset count mode, in order to obtain a minimum of 1×10^6 counts on a 128×128 matrix. The amount of blood flow shunted from infrarenal aorta to the venous system was computed by assessing the distribution of macroaggregate radioactivity; the results are expressed as

$$\frac{\text{Lung activity}}{\text{Whole body activity}} \times 100$$

Immunohistochemical staining

For histological evaluation, muscle biopsies were fixed in 2% formaldehyde and embedded in paraffin. Immunohistochemical staining of arterial vessels was performed on 2-μm-thick histological sections with mouse monoclonal antibody to α-smooth muscle actin (α-SMA) (clone 1A4; Sigma, St. Louis, MO) and goat polyclonal against platelet endothelial cell adhesion molecule-1 (PECAM1) (SC-9026; Santa Cruz Biotechnology, Santa Cruz, CA), using the VECTASTAIN Universal ABC kit, according to the manufacturer's instructions (Vector Laboratories, Burlingame, CA).

In vivo *perfusion with fluorescent microspheres*

Three animals per group were subjected to *in vivo* perfusion with a solution of orange fluorescent microspheres (FluoSpheres; Invitrogen Molecular Probes, Eugene, OR). Briefly, after anesthesia, the chest was opened and the vasculature was perfused with PBS for 3 min, followed by 20 ml of FluoSpheres (1:6 dilution of the stock), via a blunt 13-gauge needle inserted through the left ventricle into the ascending aorta. The treated muscles were removed and immediately frozen for cryosectioning. Thick (50- to 100-μm) sections were analyzed by confocal microscopy to obtain a z-stack for the three-dimensional (3D) reconstruction of the vascular network.

Statistical analysis

Changes over time were compared by one-way analysis of variance (ANOVA) for repeated measurements, followed by post hoc testing when overall significance was detected. Differences between groups were tested by two-way ANOVA. $p < 0.05$ was considered statistically significant.

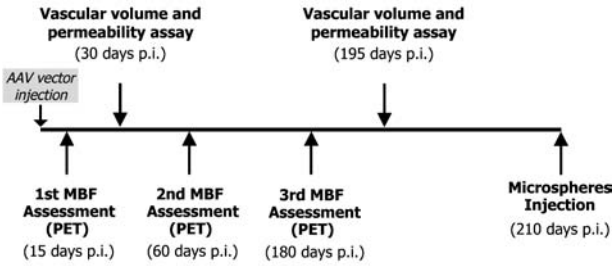

FIG. 1. Flow chart outlining the experiment. Shown schematically is the experimental protocol, including the time points of muscular blood flow (MBF) measurement, assessment of vascular volume and permeability, and quantification of flow shunting. PET, positron emission tomography; p.i., post-injection.

RESULTS

Functional evaluation of the effect of AAV-VEGF and AAV-Ang1 transduction on muscle perfusion by PET

The general outline of the whole study is shown schematically in Fig. 1. Rats were divided into four experimental groups, and all were injected via their right hindlimb with an equal amount of AAV vectors (AAV-VEGF, AAV-Ang1, AAV-VEGF + AAV-Ang1, or AAV-LacZ) and via their left hindlimb with PBS as a control; $n = 21$ per group. All the animals were then repeatedly subjected to PET imaging at various times after treatment up to 6 months, by measuring an index of muscle perfusion, bilaterally. Each PET session included two measurements of muscle blood flow (MBF), under either resting conditions or pacing-induced bilateral muscle activity. Two weeks after the last PET experiment, all the animals were injected with ^{99m}Tc-DTPA to assess vascular permeability by single-photon emission computed tomography (SPECT) and then, after an additional 2 weeks, they were evaluated for the presence of arteriovenous shunts by the injection of ^{99m}Tc-labeled microspheres into the infrarenal aorta.

A representative PET image of a rat 6 months after AAV-VEGF injection is shown in Fig. 2 together with the relative time–concentration curve of $^{13}NH_3$ uptake in the heart under resting conditions and during exercise (Fig. 2A and B, respectively). In contrast to our expectations, the prolonged expression of VEGF alone did not increase MBF as compared with the control leg under resting conditions (0.24 vs. 0.22 ml/min/g). Even more surprisingly, MBF was remarkably decreased in the VEGF-expressing leg after exercise (0.76 vs. 0.35 ml/min/g).

The results obtained from the whole set of animals are shown in Fig. 3A and B for the four experimental groups under resting and stress conditions, respectively. Left (control) limbs displayed similar MBF values in all study groups and at all time points. In contrast, a progressive decline in MBF during exercise was observed only in animals treated with VEGF up to 6 months from vector delivery. Remarkably, the simultaneous injection of AAV-VEGF and AAV-Ang1 determined a clear increase in MBF both at baseline and after exercise. This result was already evident 15 days after treatment and persisted for the whole duration of the study. Because Ang1 alone had no effect on MBF at any time point, those animals were not further considered in the subsequent experiments.

Expression of Ang1 improves functional maturation of VEGF-induced vessels

As a first step toward understanding the reason underlying the unexpected drop in MBF after AAV-VEGF transduction, the same animals were injected with ^{99m}Tc-DTPA to simultaneously analyze the effect of treatments on vascular volume and vessel permeability, the latter parameter being expressed as the product of capillary permeability (x) surface of the treated muscles. As shown in Fig. 4A and as described in Materials and Methods, two indexes of vascular volume and permeability were derived from the intercept and the slope of the line fitting the experimental data collected during the first 50 sec after DPTA injection, respectively. Intravascular blood volume was similar in both hindlimbs of the control animals (right:left hindlimb ratio: 1.1 ± 0.1 and 1.3 ± 0.2 at 1 and 6 months, respectively; Fig. 4B). In the animals treated with AAV-VEGF, the hindlimb vascular volume ratio was 2.8 ± 0.9 at 1 month, and further increased to 6.0 ± 0.9 at 6 months after injection ($p < 0.05$ and $p < 0.01$, respectively). The simultaneous expression of Ang1 clearly counteracted the VEGF-induced increase in vascular volume, because the measured hindlimb volume ratio was not significantly different from that of control animals at both time points (1.2 ± 0.2 and 1.1 ± 0.6 at 1 and 6 months, respectively). Similar observations also apply to the measurement of capillary permeability (Fig. 4C). In control animals, the permeability ratio between the two limbs was similar (0.92 ± 0.02 and 1.07 ± 0.01 at 1 and 6 months, respectively). This ratio was markedly increased in AAV-VEGF-treated rats at both 1 and 6 months after treatment (2.06 ± 0.25 and 1.5 ± 0.18, respectively; $p < 0.05$ at both time points). Again, the simultaneous delivery of AAV-Ang1 caused a significant reduction of the VEGF-induced vascular leakiness, achieving almost complete normalization after 6 months (1.35 ± 0.05 at 1 month and 1.15 ± 0.03 at 6 months, the latter being not significantly different from controls).

Effect of Ang1 on remodeling of vascular structures formed in response to VEGF

The documentation of increased intravascular volume associated with abnormal vascular leakage from the capillary microcirculation in the VEGF-treated animals possibly indicates the presence of immature vessels. To obtain further insights into the structure of the VEGF-induced vasculature, at the end of the experiment we analyzed the treated muscles in a subgroup of animals ($n = 3$ per treatment group) by immunohistochemistry. In accordance with our previous findings (Arsic *et al.*, 2003), VEGF expression, either alone or in combination with Ang1, determined the formation of a striking number of new vessels. The newly formed vasculature consisted of both capillaries and arterioles, as shown by CD31 and α-SMA staining in Fig. 5A and B, respectively. The quantification of vessels formed in response to VEGF or Ang1 alone, or in response to the combination of the two factors, is shown in Fig. 5C. Of note, no significant difference was observed in the number of capillaries and arterioles formed in response to VEGF alone or in combination with Ang1 (~4-fold- and ~9-fold increase in the number of capillaries and arterioles, respectively, over the untreated leg in both cases). Ang1 alone had no detectable angiogenic effect. Interestingly, in the muscles expressing VEGF,

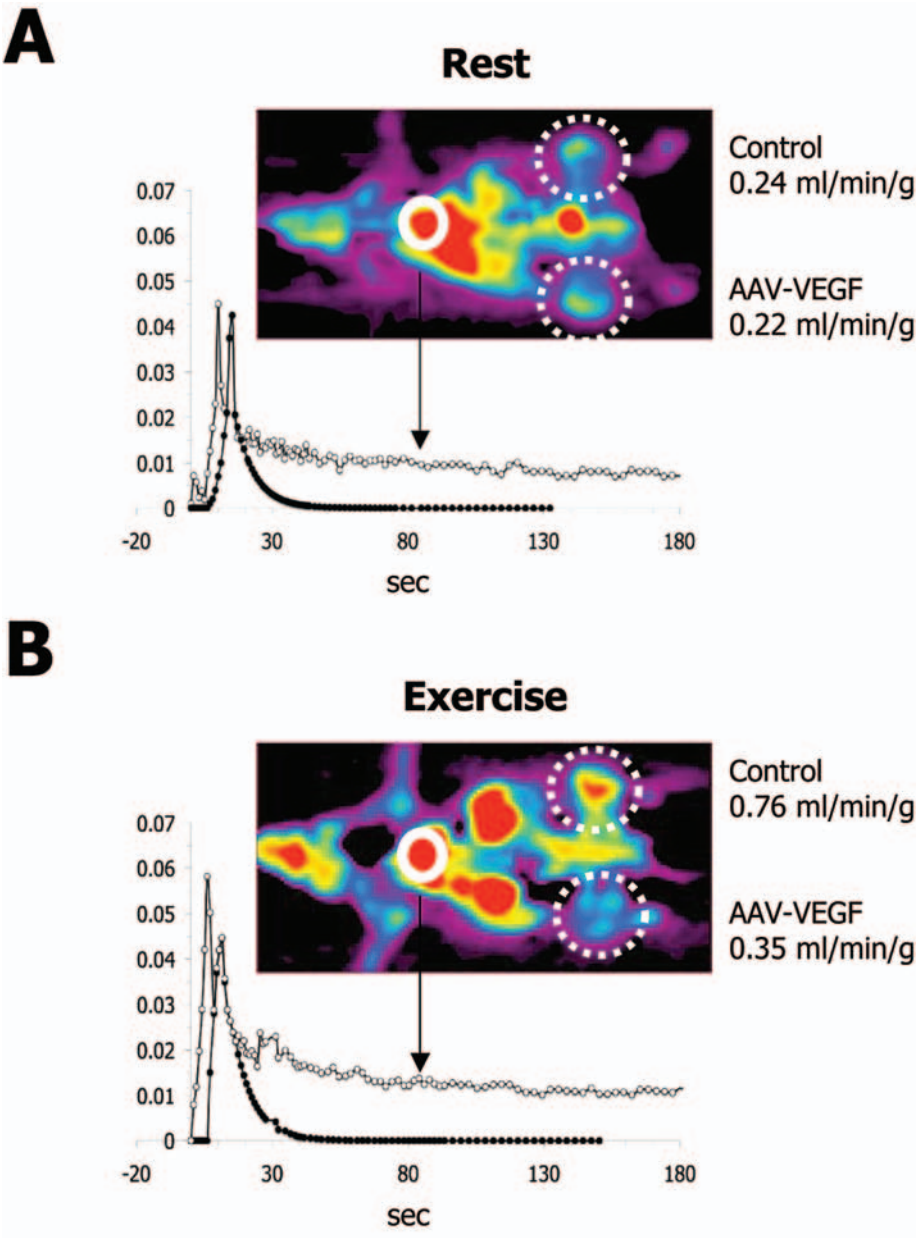

FIG. 2. Assessment of MBF by PET in a rat treated with AAV-VEGF. Shown is an example of flow measurements at rest (**A**) and during electrically induced exercise (**B**) in a rat treated with AAV-VEGF. In the graphs below each image, the time–concentration curve of ^{13}N-labeled ammonia in the heart region is shown (open circles) together with the γ-variate function used for integration (solid circles). MBF for each leg is indicated on the right side of each picture.

we also observed the formation of several abnormal vascular structures invading the muscle parenchyma (Fig. 5E). Most of these vascular lacunae appeared to be filled with erythrocytes, an observation indicating their connection to the systemic circulation. In contrast, in the muscles coinjected with AAV-VEGF and AAV-Ang1, these vascular lacunae were only occasionally detected and were always of small size.

To obtain final proof of the connection of the newly formed vascular structures with the systemic circulation, as well as to reconstruct the vascular network of the differently treated muscles, a suspension of small fluorescent microspheres (diameter, 0.2 μm) was systemically injected through the left ventricle. After sacrifice, thick (100-μm) muscle sections were obtained and at least 20 confocal planes were scanned for 3D image reconstruction. A planar view of 3D reconstructions of thick muscle sections is shown in Fig. 5F for the various experimental groups. The vessels formed in response to VEGF were found to be abnormally large and poorly organized, sometimes invading the muscle fiber parenchyma. In contrast, more structured vessels were evident when Ang1 was expressed together with VEGF in the skeletal muscle. Of interest, in the VEGF plus Ang1-treated animals, each muscle fiber appeared to be surrounded by a dense network of capillaries, possibly indicating an increase in the exchange surface between muscle and endothelial cells.

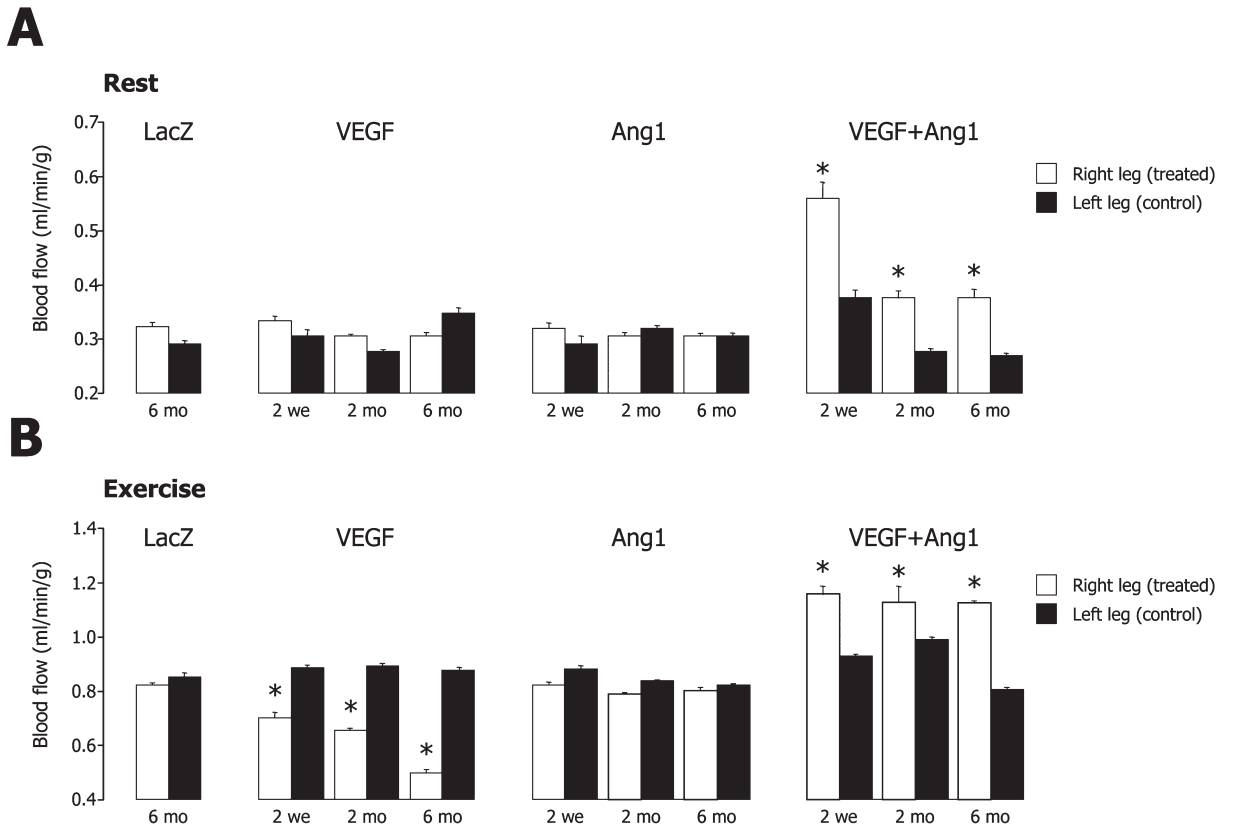

FIG. 3. Assessment of MBF by PET in all experimental groups. Shown is MBF at rest (**A**) and during exercise (**B**) in the four experimental groups, as indicated (means ± SD). Solid and open columns show values for the left (control) and right (treated) limbs, respectively. Asterisks indicate statistical significance.

VEGF triggers the formation of arteriovenous shunts that are markedly reduced on coexpression of angiopoietin-1

The abnormal size and shape of the vessels formed in response to VEGF, together with the formation of vascular lacunae, might represent the anatomical basis for the occurrence of arteriovenous shunts that might bypass the microcirculation and thus explain the poor functionality of the newly formed vasculature. To specifically assess this hypothesis, a bolus of radioactive macroaggregates with a diameter range of 25–200 μm was injected into the abdominal aorta and the amount of radioactive spheres not trapped in the capillary bed and shunted to the lungs was determined by whole body acquisition with a γ-camera. As shown in representative animals in Fig. 6A and as quantified in Fig. 6B for all experimental groups, the presence of an important arteriovenous shunting activity was observed as a consequence of VEGF expression (11.3 ± 1.2% of abdominal aorta flow shunted to lungs in the VEGF group vs. 3.6 ± 0.4% in the control group; $p < 0.05$). The coinjection of AAV-Ang1 markedly reduced this effect (6.2 ± 0.6, $p < 0.05$ vs. both VEGF and control).

DISCUSSION

In this study we took advantage of some of the imaging techniques already validated in the clinic to assess the functional consequence of the neovascularization driven by VEGF single-gene transfer, or by the combined delivery of the VEGF and Ang1 genes. The most striking result of this study is that the continuous expression of VEGF in skeletal muscle, despite inducing a massive increase in vessel density and tissue blood pool, does not improve functional tissue perfusion at rest and even worsens perfusion during exercise. We provide at least two mechanisms to explain the poor functionality of the VEGF-induced blood vessels, namely that the VEGF-induced vasculature is abnormally leaky and that it involves the formation of arteriovenous shunts that exclude the microcirculation.

The permeabilizing activity of VEGF, 50,000-fold greater than histamine, is widely recognized (Senger *et al*., 1983) and has been attributed to the induction of endothelial fenestrations. Our data confirm this effect by showing that, *in vivo*, treatment with VEGF causes an increase in vascular permeability that is already evident 1 month after injection and persists for at least 6 months. Given the potency of the permeabilizing effect of VEGF—which appears at doses probably lower than those sufficient to promote neoangiogenesis (Eriksson *et al*., 2003)—it is surprising that the occurrence of edema or of its related effects has never emerged in clinical trials that have used this factor (Cao *et al*., 2005). This probably indicates that an effective dose of VEGF has never been reached in these studies, thus also explaining their poor outcome in terms of neovascularization. The failure of most of these studies likely depends on the gene delivery systems that were employed, namely the injec-

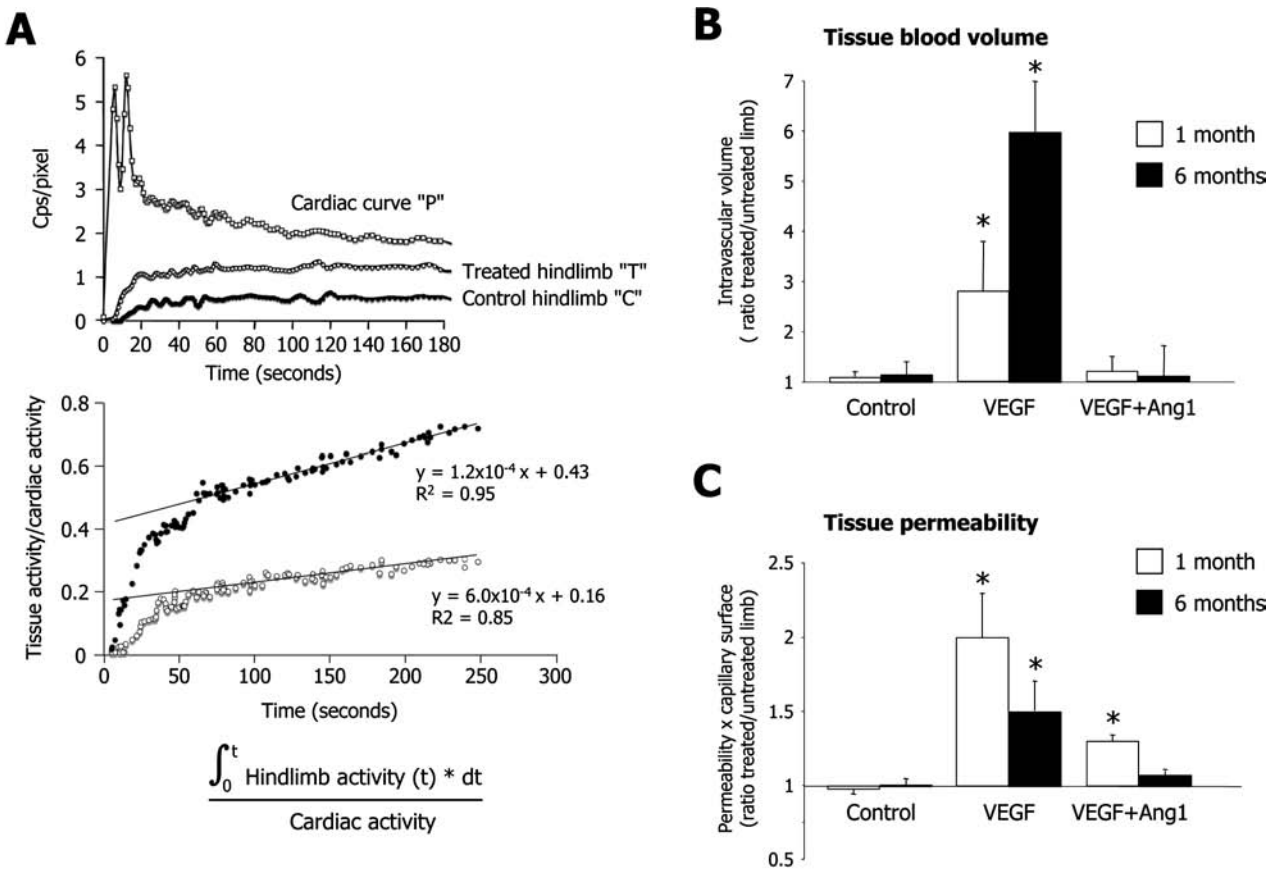

FIG. 4. Assessment of vascular volume and permeability by single-photon emission computed tomography (SPECT). (**A**) *Top*: Representative time–activity curve of ^{99m}Tc-DTPA on regions of interest (ROIs) drawn on heart (open squares), control (solid circles), and treated (open circles) hindlimb, respectively, 1 month after injection of AAV-VEGF. The increase in muscular tracer uptake in the treated limb is evident. *Bottom*: Analysis plot showing that the regression line of the experimental point in the treated region is characterized by a larger intercept and a steeper slope, indicative of increased blood content and greater permeability, respectively, with respect to the control hindlimb; also see Materials and Methods. (**B** and **C**) Effect of treatments on blood volume (**B**) and (permeability × surface) product (**C**) in the different experimental groups, 1 and 6 months after injection. Data represent means ± SD; asterisks indicate statistical significance. Cps, counts per second.

tion of plasmid DNA or the transduction with first-generation adenoviral vectors. Indeed, the former procedure is fraught by low transduction efficiency, whereas the latter suffers from the short duration of transgene expression (usually less than 2–3 weeks) and by the induction of a strong inflammatory and immune response. In contrast, gene delivery with AAV vectors, as in this study, leads to efficiency and stable gene expression over time (Monahan and Samulski, 2000).

Besides permeability, here we also report, for the first time, that the vasculature formed on the prolonged expression of VEGF also involves the pathological formation of arteriovenous shunts that exclude the microcirculation. Although our study does not allow a precise estimation of the diameter of these VEFG-induced shunts, they are likely larger than 25 μm (the smallest size of the injected particles). This size is indeed consistent with the dimension of the VEGF-induced vascular lacunae, which most likely represent the anatomical substrate of the arteriovenous shunts. The fact that these vascular structures are actually filled with erythrocytes is in perfect agreement with the marked increase in the blood pool in the treated muscles, as measured by ^{99m}Tc-DTPA here or, previously, by the use of fluorescent microspheres (Arsic *et al*., 2003). However, despite this apparent increase in blood content of the VEGF-treated muscles, the extremely low resistance to flow of the arteriovenous shunts determines a preferential redirection of blood flow excluding the microcirculation, with a subsequent "stealing" effect on tissue perfusion that becomes particular evident during exercise.

These results add support to the concern, raised by several investigators, that a VEGF-based gene therapy approach may lead to abnormal vessel growth, including the formation of hemangiomas and glomeruloid bodies, without improving functional perfusion (Lee *et al*., 2000; Schwarz *et al*., 2000; Springer *et al*., 2003). This condition is indeed reminiscent of the tumor-associated vasculature, in which the unregulated expression of VEGF determines the formation of abnormally leaky vessels and the occurrence of significant blood shunting to the venous system (Leung *et al*., 1995; Weis and Cheresh, 2005).

In contrast to VEGF alone, a combination approach, in which both VEGF and Ang1 are simultaneously delivered to the skeletal muscle, appears to be effective in improving effective muscle perfusion under resting conditions and after exercise. With the caveat that the kinetics and extent of these results might vary under ischemic conditions, this conclusion appears of par-

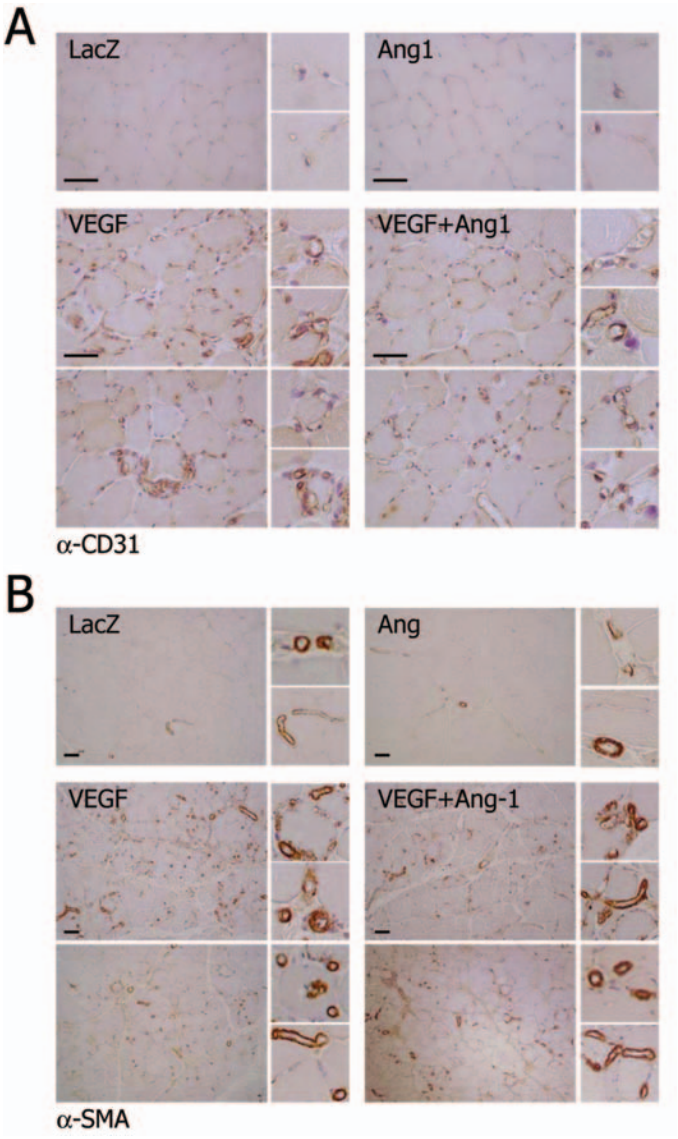

FIG. 5. Vascular structures formed in response to AAV-VEGF and AAV-Ang1 transduction. (**A**) Immunostaining of muscle sections of animals treated with the various vector combinations, as indicated, using an antibody against the endothelial cell marker CD31. Higher magnifications are shown at the right side of each panel. Scale bars: 100 μm. (**B**) Same as in (**A**), using an antibody against α-smooth muscle actin (α-SMA) to visualize arterial vessels. Scale bars: 100 μm. (**C**) Quantification of CD31-positive capillary vessels in muscles injected with the indicated vectors. Capillaries were defined as 5- to 10-μm-diameter vessels surrounded only by CD31-positive cells. Counts were obtained from both the leg injected with the angiogenic vector (or AAV-LacZ) and the contralateral leg, and are expressed as a ratio between the two measurements (means $\pm$ SD). The quantifications were carried out by three independent investigators, blinded for experimental procedures, who observed 10 different sections from 3 animals per group. (**D**) Quantification of α-SMA-positive arterioles. Quantifications were performed, and are expressed, as in (**C**). (**E**) Formation of aberrant vascular structures on VEGF expression. Sustained VEGF overexpression alone determined the formation of large vascular spaces (vascular lacunae) filled with erythrocytes (indicated by arrows). Scale bars: 100 μm. (**F**) Confocal microscopy reconstruction of the vascular network induced by AAV-VEGF or AAV-VEGF plus AAV-Ang1 transduction, after *in vivo* perfusion of the animals with a suspension of fluorescent microspheres. Compared with normal or LacZ-treated muscles (*top*), fibers of the AAV-VEGF-injected muscles appeared surrounded and partially substituted by large and poorly organized vascular structures (*middle*). When AAV-Ang1 was coinjected with AAV-VEGF, the surrounding vessels appeared of normal morphology, although still larger than in controls. Scale bar: 100 μm.

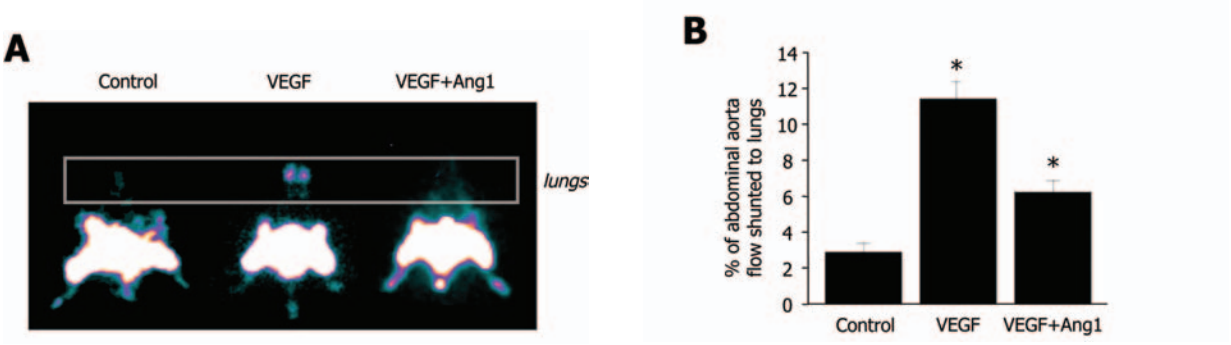

FIG. 6. Evaluation of arteriovenous shunting, using ^{99m}Tc-labeled microspheres. (**A**) SPECT visualization of the distribution of radioactive macroaggregates injected into the abdominal aorta. A representative animal for each experimental group is shown. The region of the body corresponding to the lungs is included in the outlined rectangle. (**B**) Quantification of the percentage of aortic blood shunted to the lungs of animals of the various experimental groups. The results indicate the presence of arteriovenous shunts in the animals treated with AAV-VEGF, which is significantly decreased on Ang1 coexpression ($p < 0.05$). Data are expressed as means $\pm$ SD. The asterisks denote statistical significance.

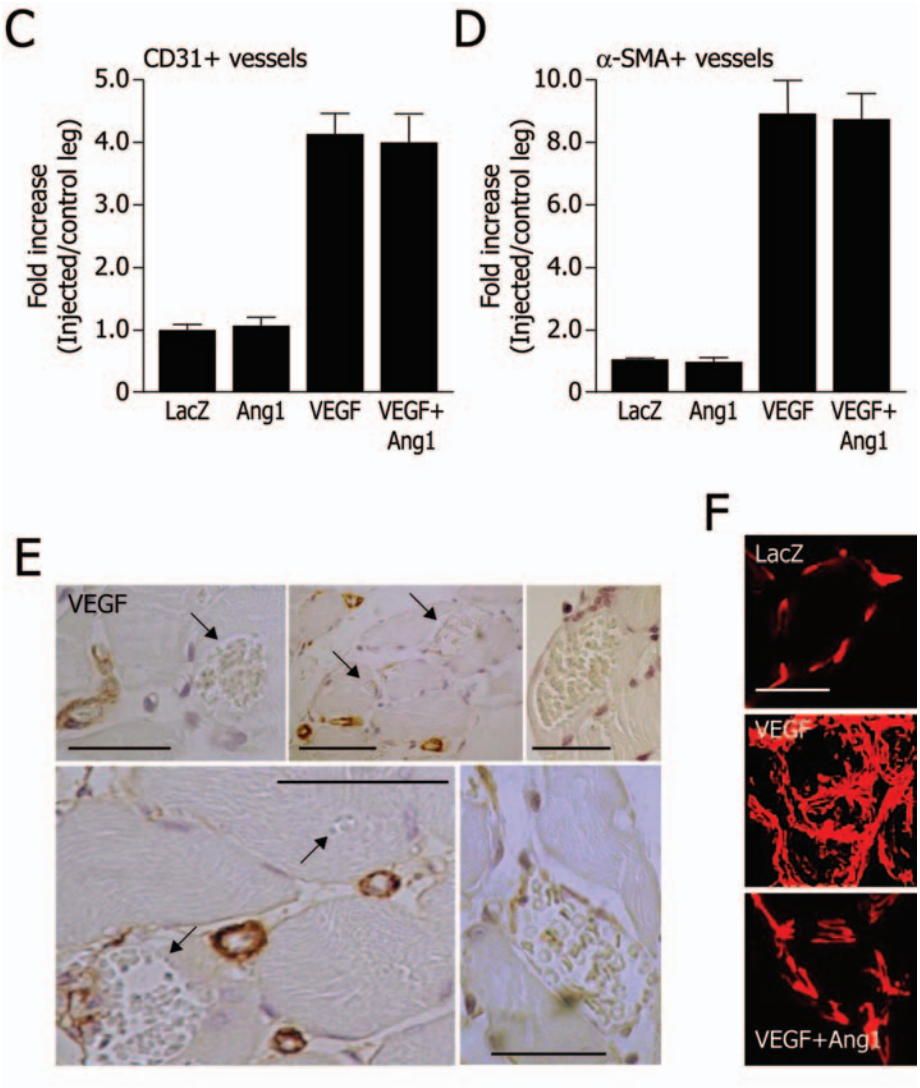

FIG. 5. (*Continued*).

ticular importance for any future clinical application of therapeutic angiogenesis, because it suggests that more than one factor is required for proper new blood vessel formation. Different molecular mechanisms might support the favorable effects of Ang1 on vessel maturation and function, including the recruitment of pericytes (Dumont *et al*., 1994; Suri *et al*., 1996) or mesenchymal precursors (Metheny-Barlow *et al*., 2004), the strengthening of intercellular junctions between adjacent endothelial cells (Gamble *et al*., 2000), and the direct interference with the intracellular signaling pathways responsible for VEGF-triggered vascular leakiness (Jho *et al*., 2005).

From a clinical perspective, our results clearly indicate that morphological evidence of angiogenesis, even in the presence of a documented increase in vascular volume, does not necessarily account for improved functional perfusion. This observation emphasizes the importance of functional and noninvasive tests to assess the real efficacy of any angiogenic factor, and to accurately study all the possible side effects that might arise as consequence of its overexpression. Collectively, our results challenge the value of VEGF single-gene transfer to induce therapeutic angiogenesis in patients, and prompts the design of new clinical experimentations based on the delivery of cytokine cocktails that might be effective in the generation of a functionally competent neovasculature.

ACKNOWLEDGMENTS

This work was supported by grants from the FIRB program of the Ministero dell'Istruzione, Università e Ricerca, Italy and from the Fondazione Cassa di Risparmio of Trieste, Italy. The authors are grateful to Marina Dapas for excellent technical support and to Suzanne Kerbavcic for editorial assistance.

AUTHOR DISCLOSURE STATEMENT

No competing financial interests exist.

REFERENCES

ARSIC, N., ZENTILIN, L., ZACCHIGNA, S., SANTORO, D., STANTA, G., SALVI, A., SINAGRA, G., and GIACCA, M. (2003). Induction of functional neovascularization by combined VEGF and angiopoietin-1 gene transfer using AAV vectors. Mol. Ther. **7,** 450–459.

ARSIC, N., ZACCHIGNA, S., ZENTILIN, L., RAMIREZ-CORREA, G., PATTARINI, L., SALVI, A., SINAGRA, G., and GIACCA, M. (2004). Vascular endothelial growth factor stimulates skeletal muscle regeneration *in vivo*. Mol. Ther. **10,** 844–854.

BELLINA, C.R., PARODI, O., CAMICI, P., SALVADORI, P.A., TADDEI, L., FUSANI, L., GUZZARDI, R., KLASSEN, G.A., L'ABBATE, A.L., and DONATO, L. (1990). Simultaneous *in vitro* and *in vivo* validation of nitrogen-13-ammonia for the assessment of regional myocardial blood flow. J. Nucl. Med. **31,** 1335–1343.

CAO, Y., HONG, A., SCHULTEN, H., and POST, M.J. (2005). Update on therapeutic neovascularization. Cardiovasc. Res. **65,** 639–648.

DEODATO, B., ARSIC, N., ZENTILIN, L., GALEANO, M., SANTORO, D., TORRE, V., ALTAVILLA, D., VALDEMBRI, D., BUSSOLINO, F., SQUADRITO, F., and GIACCA, M. (2002). Recombinant AAV vector encoding human VEGF165 enhances wound healing. Gene Ther. **9,** 777–785.

DUMONT, D.J., GRADWOHL, G., FONG, G.H., PURI, M.C., GERTSENSTEIN, M., AUERBACH, A., and BREITMAN, M.L. (1994). Dominant-negative and targeted null mutations in the endothelial receptor tyrosine kinase, Tek, reveal a critical role in vasculogenesis of the embryo. Genes Dev. **8,** 1897–1909.

ERIKSSON, A., CAO, R., ROY, J., TRITSARIS, K., WAHLESTEDT, C., DISSING, S., THYBERG, J., and CAO, Y. (2003). Small GTP-binding protein Rac is an essential mediator of vascular endothelial growth factor-induced endothelial fenestrations and vascular permeability. Circulation **107,** 1532–1538.

FERRARA, N. (2005). VEGF as a therapeutic target in cancer. Oncology **69**(Suppl. 3)**,** 11–16.

FERRARA, N., and ALITALO, K. (1999). Clinical applications of angiogenic growth factors and their inhibitors. Nat. Med. **5,** 1359–1364.

FERRARA, N., GERBER, H.P., and LECOUTER, J. (2003). The biology of VEGF and its receptors. Nat. Med. **9,** 669–676.

GALEANO, M., DEODATO, B., ALTAVILLA, D., CUCINOTTA, D., ARSIC, N., MARINI, H., TORRE, V., GIACCA, M., and SQUADRITO, F. (2003). Adeno-associated viral vector mediated human vascular endothelial growth factor gene transfer stimulates angiogenesis and wound healing in the genetically diabetic mouse. Diabetologia **46,** 546–555.

GAMBLE, J.R., DREW, J., TREZISE, L., UNDERWOOD, A., PARSONS, M., KASMINKAS, L., RUDGE, J., YANCOPOULOS, G., and VADAS, M.A. (2000). Angiopoietin-1 is an antipermeability and anti-inflammatory agent *in vitro* and targets cell junctions. Circ. Res. **87,** 603–607.

JHO, D., MEHTA, D., AHMMED, G., GAO, X.P., TIRUPPATHI, C., BROMAN, M., and MALIK, A.B. (2005). Angiopoietin-1 opposes VEGF-induced increase in endothelial permeability by inhibiting TRPC1-dependent Ca^{2+} influx. Circ. Res. **96,** 1282–1290.

LEE, R.J., SPRINGER, M.L., BLANCO-BOSE, W.E., SHAW, R., URSELL, P.C., and BLAU, H.M. (2000). VEGF gene delivery to myocardium: Deleterious effects of unregulated expression. Circulation **102,** 898–901.

LEUNG, T.W., LAU, W.Y., HO, S.K., WARD, S.C., CHOW, J.H., CHAN, M.S., METREWELI, C., JOHNSON, P.J., and LI, A.K. (1995). Radiation pneumonitis after selective internal radiation treatment with intraarterial ^{90}yttrium-microspheres for inoperable hepatic tumors. Int. J. Radiat. Oncol. Biol. Phys. **33,** 919–924.

LOSORDO, D.W., VALE, P.R., SYMES, J.F., DUNNINGTON, C.H., ESAKOF, D.D., MAYSKY, M., ASHARE, A.B., LATHI, K., and ISNER, J.M. (1998). Gene therapy for myocardial angiogenesis: Initial clinical results with direct myocardial injection of phVEGF165 as sole therapy for myocardial ischemia. Circulation **98,** 2800–2804.

METHENY-BARLOW, L.J., TIAN, S., HAYES, A.J., and LI, L.Y. (2004). Direct chemotactic action of angiopoietin-1 on mesenchymal cells in the presence of VEGF. Microvasc. Res. **68,** 221–230.

MONAHAN, P.E., and SAMULSKI, R.J. (2000). AAV vectors: Is clinical success on the horizon? Gene Ther. **7,** 24–30.

PETERS, A.M., BROWN, J., HARTNELL, G.G., MYERS, M.J., HASKELL, C., and LAVENDER, J.P. (1987). Non-invasive measurement of renal blood flow with ^{99m}Tc DTPA: Comparison with radiolabelled microspheres. Cardiovasc. Res. **21,** 830–834.

POST, M., and WALTENBERGER, J. (2005). Modulation of growth factor action in the cardiovascular system. Cardiovasc. Res. **65,** 547–549.

SCHWARZ, E.R., SPEAKMAN, M.T., PATTERSON, M., HALE, S.S., ISNER, J.M., KEDES, L.H., and KLONER, R.A. (2000). Evaluation of the effects of intramyocardial injection of DNA expressing vascular endothelial growth factor (VEGF) in a myocardial infarction model in the rat: Angiogenesis and angioma formation. J. Am. Coll. Cardiol. **35,** 1323–1330.

SENGER, D.R., GALLI, S.J., DVORAK, A.M., PERRUZZI, C.A., HARVEY, V.S., and DVORAK, H.F. (1983). Tumor cells secrete a vascular permeability factor that promotes accumulation of ascites fluid. Science **219,** 983–985.

SIDDIQUI, A.J., BLOMBERG, P., WARDELL, E., HELLGREN, I., ESKANDARPOUR, M., ISLAM, K.B., and SYLVEN, C. (2003). Combination of angiopoietin-1 and vascular endothelial growth factor gene therapy enhances arteriogenesis in the ischemic myocardium. Biochem. Biophys. Res. Commun. **310,** 1002–1009.

SPRINGER, M.L., OZAWA, C.R., BANFI, A., KRAFT, P.E., IP, T.K., BRAZELTON, T.R., and BLAU, H.M. (2003). Localized arteriole formation directly adjacent to the site of VEGF induced angiogenesis in muscle. Mol. Ther. **7,** 441–449.

SURI, C., JONES, P.F., PATAN, S., BARTUNKOVA, S., MAISONPIERRE, P.C., DAVIS, S., SATO, T.N., and YANCOPOULOS, G.D. (1996). Requisite role of angiopoietin-1, a ligand for the TIE2 receptor, during embryonic angiogenesis. Cell **87,** 1171–1180.

THURSTON, G., SURI, C., SMITH, K., MCCLAIN, J., SATO, T.N., YANCOPOULOS, G.D., and MCDONALD, D.M. (1999). Leakage-resistant blood vessels in mice transgenically overexpressing angiopoietin-1. Science **286,** 2511–2514.

WEIS, S.M., and CHERESH, D.A. (2005). Pathophysiological consequences of VEGF induced vascular permeability. Nature **437,** 497–504.

YLA-HERTTUALA, S., MARKKANEN, J.E., and RISSANEN, T.T. (2004). Gene therapy for ischemic cardiovascular diseases: Some lessons learned from the first clinical trials. Trends Cardiovasc. Med. **14,** 295–300.

ZACCHIGNA, S., PAPA, G., ANTONINI, A., NOVATI, F., MOIMAS, S., CARRER, A., ARSIC, N., ZENTILIN, L., VISINTINI, V., PASCONE, M., and GIACCA, M. (2005). Improved survival of ischemic cutaneous and musculocutaneous flaps after vascular endothelial growth factor gene transfer using adeno-associated virus vectors. Am. J. Pathol. **167,** 981–991.

ZENTILIN, L., TAFURO, S., ZACCHIGNA, S., ARSIC, N., PATTARINI, L., SINIGAGLIA, M., and GIACCA, M. (2006). Bone marrow mononuclear cells are recruited to the sites of VEGF-induced neovascularization but are not incorporated into the newly formed vessels. Blood **107,** 3546–3554.

Address reprint requests to:
Dr. Mauro Giacca
ICGEB Trieste
Padriciano, 99
34012 Trieste, Italy

E-mail: giacca@icgeb.org

Received for publication October 27, 2006; accepted after revision April 6, 2007.

Published online: May 23, 2007.